

Superconducting phase fluctuations in $\text{SmFeAsO}_{0.8}\text{F}_{0.2}$ from diamagnetism at low magnetic field above T_c

G. Prando,^{1,2} A. Lascialfari,^{1,3,4} A. Rigamonti,¹ L. Romanó,⁵ S. Sanna,¹ M. Putti,⁶ M. Tropeano^{6,7}

¹*Department of Physics “A. Volta,” University of Pavia-CNISM, I-27100 Pavia, Italy*

²*Department of Physics “E. Amaldi,” University of Roma Tre-CNISM, I-00146 Roma, Italy*

³*Department of Molecular Sciences Applied to Biosystems, University of Milano, I-20134 Milano, Italy*

⁴*Centro S3, CNR-Istituto di Nanoscienze, I-41125 Modena, Italy*

⁵*Department of Physics, University of Parma-CNISM, I-43124 Parma, Italy*

⁶*CNR-SPIN and University of Genova, I-16146 Genova, Italy and*

⁷*Columbus Superconductors SpA, I-16133 Genova, Italy*

Superconducting fluctuations (SF) in $\text{SmFeAsO}_{0.8}\text{F}_{0.2}$ (characterized by superconducting transition temperature $T_c \simeq 52.3$ K) are investigated by means of isothermal high-resolution dc magnetization measurements. The diamagnetic response above T_c to magnetic fields up to 1 T is similar to that previously reported for underdoped cuprate superconductors and justified in terms of metastable superconducting islands of non-zero order parameter lacking long-range coherence because of strong phase fluctuations. In the high-field regime ($H \gtrsim 1.5$ T) scaling arguments predicted on the basis of the Ginzburg-Landau theory for conventional SF are confirmed, at variance with what is observed in the low-field regime. This fact shows that two different phenomena are simultaneously present in the fluctuating diamagnetism, namely the phase SF of novel character and the conventional SF. High magnetic fields ($1.5 \text{ T} \lesssim H \ll H_{c2}$) are found to suppress the former while leaving unaltered the latter.

PACS numbers: 74.40.-n, 74.20.De, 74.70.Xa

I. INTRODUCTION

High-temperature superconductivity in Fe-based oxy-pnictides has aroused strong interest among condensed matter physicists after its discovery in 2008.¹ In spite of the huge amount of both theoretical and experimental activities^{2,3} several questions are still open, particularly regarding the pairing mechanism. The symmetry of the order parameter has been investigated by means of Josephson tunneling and ARPES experiments. Results show that in Fe-based superconductors (both in doped REFeAsO , where RE stands for rare-earth ion, and doped $(\text{Ba,Sr})\text{Fe}_2\text{As}_2$ compounds, belonging to the so-called 1111 and 122 families respectively) s -wave singlet superconductivity is at work.^{4,5} A multi-band scenario has been proposed, where the appearance of two different superconducting gaps seems to characterize Fe-based pnictide materials. BCS theory anyway cannot account for either the high values of T_c or the temperature dependence of the superconducting gaps, similarly to the case of MgB_2 .⁶ Eliashberg theory for strong-coupling resulting in an interband s^\pm -wave model^{7,8} is needed in order to account for the experimental results from Josephson tunneling on $\text{NdFeAsO}_{0.88}\text{F}_{0.12}$ ⁴ and from point-contact Andreev-reflection spectroscopy on $\text{SmFeAsO}_{1-x}\text{F}_x$.⁹

Besides these similarities with s -wave superconductors and with MgB_2 , many experimental evidences emphasize affinities of Fe-based oxy-pnictides with the cuprate high-temperature superconductors (HTSC). By means of magnetoresistivity¹⁰ and ac susceptibility¹¹ it has been pointed out that the features of vortex dynamics in $\text{SmFeAsO}_{1-x}\text{F}_x$ can be mapped onto models successfully applied to cuprate materials,¹² as, for instance,

the thermally-activated flux flow of vortex lines. Moreover, scaling arguments from vortex-glass theory developed for $I-V$ characteristics of cuprates^{13,14} were found to describe experimental data also in $\text{SmFeAsO}_{0.85}$.¹⁰ The existence of a pseudo-gap precursor state also in $\text{SmFeAsO}_{1-x}\text{F}_x$, finally, has been suggested by different experimental evidences.¹⁵⁻¹⁹

Small coherence lengths, reduced carriers density, high transition temperatures and marked anisotropy are all factors causing a strong enhancement of superconducting fluctuations (SF).²⁰⁻²² The generation of fluctuating Cooper pairs above T_c results in the appearance of a Langevin-type diamagnetic contribution to the magnetization $-M_{dia}(T, H)$ existing side by side with the paramagnetic contribution from fermionic carriers. Since the size $\xi(T)$ of the fluctuating pairs grows when T approaches the transition temperature T_c from above, $|M_{dia}(T, H)|$ should diverge near the transition for any small fixed magnetic field, being zero for $H = 0$ Oe. On the other hand, it is evident that very strong magnetic fields, comparable to $H_{c2}(0)$, must suppress SF. Thus, the isothermal magnetization curve $-M_{dia}(\bar{T}, H)$ (\bar{T} is a fixed temperature) has to exhibit an upturn. The value of the upturn field H_{up} in the magnetization curves can approximately be considered inversely proportional to the coherence length.²⁰⁻²² Thus, in optimally doped cuprates, H_{up} is expected at very strong magnetic fields. At variance, in underdoped superconducting cuprates, the magnetization curves above T_c evidence an upturn for $H \ll H_{c2}(0)$.^{23,24}

As shown in the following, similar effects have been found in Fe-based oxy-pnictides belonging to the $\text{REFeAsO}_{1-x}\text{F}_x$ family, evidencing a further anal-

ogy with cuprate superconductors. SF in Fe-based oxy-pnictides have already been theoretically discussed.²⁵ Calorimetric measurements performed on $\text{SmFeAsO}_{0.85}\text{F}_{0.15}$ single-crystals have been recently interpreted in terms of Ginzburg-Landau SF.²⁶ Furthermore, a magnetic investigation of $\text{Ba}_{1-x}\text{K}_x\text{Fe}_2\text{As}_2$ single-crystals has been carried out in the high-field regime²⁷ and classical Ginzburg-Landau scaling has been observed. Until now, to our knowledge, no claim of non-classical SF in Fe-based oxy-pnictide superconductors has been reported yet.

This paper deals with high-resolution magnetization measurements above T_c in $\text{SmFeAsO}_{0.8}\text{F}_{0.2}$. The observed phenomenology at low magnetic fields $H \lesssim 1$ T can be well-described in terms of the superconducting phase fluctuation model, confirming an analogy of $\text{SmFeAsO}_{0.8}\text{F}_{0.2}$ with underdoped cuprate superconductors. In this picture, extra-diamagnetism arises above T_c due to the appearance of mesoscopic superconducting “islands” with nonzero order parameter at frozen amplitude lacking of coherence due to marked phase fluctuations.^{28,29} In the high-field range $1.5 \text{ T} \lesssim H \ll H_{c2}$ the suppression of superconducting phase fluctuations is found to leave unaltered the classical Ginzburg-Landau fluctuations, making scaling arguments applicable.

II. EXPERIMENTAL

Powders of $\text{SmFeAsO}_{0.8}\text{F}_{0.2}$ were prepared by solid state reaction at ambient pressure from Sm, As, Fe, Fe_2O_3 and FeF_2 .³⁰ SmAs was first synthesized from pure elements in an evacuated, sealed glass tube at a maximum temperature of 550°C . The final sample was synthesized by mixing SmAs, Fe, Fe_2O_3 and FeF_2 powders in stoichiometric proportions, using uniaxial pressing to obtain pellets and then thermal treating in an evacuated, sealed quartz tube at 1000°C for 24 hours, followed by furnace cooling. The sample was analyzed by powder X-ray diffraction in a Guinier camera, with Si as internal standard. The powder pattern showed the sample to be nearly single phase with two weak extra lines at low angle attributable to SmOF. The lattice parameters $a = 3.930(1) \text{ \AA}$ and $c = 8.468(2) \text{ \AA}$ have been derived, in agreement with data reported elsewhere.³¹ The magnetic characterization of the sample was reported in a previous paper, together with a ^{19}F -NMR investigation allowing one to infer that the pairing mechanism is uncorrelated with fluctuating Sm^{3+} magnetic moments.³²

The magnetization M measurements were carried out by means of Quantum Design MPMS-XL7 SQUID magnetometer. The experimental data were collected both in zero-field-cooled (ZFC) and field-cooled (FC) conditions. In ZFC measurements, the magnetic field is applied at a given temperature after cooling the sample across the superconducting critical temperature T_c in zero applied field. In FC measurements the magnetic field is applied

at temperatures $T \gg T_c$.

III. SUPERCONDUCTING FLUCTUATIONS VS. PRECURSOR DIAMAGNETISM

The response of superconducting materials to the application of magnetic fields at $T \gtrsim T_c$ shows a diamagnetic contribution to the magnetization (M_{dia}) superimposed on the Pauli-like paramagnetic term due to fermionic carriers.^{21,22} This effect may be due to different phenomenologies and could arise from different origins, as explained in detail below.

A. Ginzburg-Landau superconducting fluctuations

In most cases, as in conventional metallic superconductors, cuprate materials and MgB_2 , the appearance of a diamagnetic term at $T \gtrsim T_c$ can be associated with fluctuations of the order parameter $\psi = |\psi|e^{i\theta}$ (superconducting fluctuations, SF).^{23,33–37} In particular, in the classical Ginzburg-Landau framework of second-order phase transitions, one has to take into account fluctuations of the amplitude of ψ around its equilibrium value $|\psi| = 0$, leading the quantity $\sqrt{\langle|\psi|^2\rangle}$ to assume non-zero values for $T \gtrsim T_c$.^{21,22}

The Ginzburg-Landau picture must be corrected to take into account the field effects on the Cooper pairs and the anisotropic free-energy functional. In three-dimensional (3D) superconductors for $T \simeq T_c$ one has $M_{dia} \propto \sqrt{H}$ (Prange regime)^{21,22} and by increasing the field saturation of $|M_{dia}|$ is expected. Furthermore, isothermal M_{dia}/\sqrt{H} vs. H curves are expected to cross at $T_c(H = 0)$.^{33,38}

In optimally-doped cuprate superconductors, the fluctuating diamagnetic contribution is expected to be suppressed by the application of magnetic fields $H \sim H_{c2}$. This corresponds to the appearance of an upturn field H_{up} defined as the value of magnetic field at which $|M_{dia}|$ starts to decrease on increasing H , as already mentioned. For optimally-doped cuprate HTSC, the upturn field could occur at very high values, typically of the order of tens of Teslas. In fact, H_{up} can be crudely justified by assuming a first order correction in which the fluctuations-induced evanescent superconducting droplets are spherical, with a diameter d of the order of the coherence length $\xi(T)$. If $d \ll \xi(T)$, the zero-dimensional approximation can be used³⁹ where the order parameter is no longer dependent on spatial degrees of freedom. In this approach, the value of the upturn field H_{up} becomes inversely proportional to the square of the coherence length $\xi(T \rightarrow 0)$: $H_{up} = \epsilon\Phi_0/\xi^2(0)$, where $\epsilon = (T - T_c)/T_c$ and $\Phi_0 = hc/2e = 2.0679 \cdot 10^{-7} \text{ G cm}^2$ corresponds to the flux quantum. In conventional BCS superconductors or in MgB_2 , H_{up} is rather small (typically around 50 to 100 Oe) while in HTSC the upturn in M_{dia} vs. H could be detected only at very high fields and in optimally doped

YBa₂Cu₃O_{6+δ} (YBCO) no upturn in M_{dia} has been observed up to 7 Teslas.^{24,38,40,41}

B. Phase fluctuations and precursor diamagnetism

At variance with the findings recalled above, underdoped cuprate materials display much richer phenomenologies than the optimally doped ones.^{24,40-43} In particular, upturn fields $H_{up} \simeq 10 - 1000$ Oe have been evidenced. This phenomenon can be justified by taking into account the fluctuations of the phase of the superconducting order parameter in mesoscopic “islands”, the

long-range superconductivity being prevented by the lack of coherence due to marked phase fluctuations.^{28,29,44} The existence of these islands is supported by scanning microscopy, at least in La_{2-x}Sr_xCuO₄ (LSCO) and in Bi-based cuprates,⁴⁵⁻⁴⁷ and by the detection of a large Nernst signal above T_c .⁴⁸ The fluctuations of the order parameter phase imply the presence of thermally induced vortices which add to those generated by the magnetic field.

The starting point to derive the magnetic susceptibility is the Lawrence-Doniach-like functional for a layered system:²¹

$$\mathcal{F}_{LD}[\theta] = \frac{1}{s} \sum_l \int d^2\mathbf{r} \left\{ J_{\parallel} \left(\nabla_{\parallel} \theta - \frac{i2e}{\hbar c} A_{\parallel} \right)^2 + J_{\perp} [1 - \cos(\theta_{l+1} - \theta_l)] \right\} \quad (1)$$

where $|\psi|^2$ is frozen at a constant value and only the dependence on the phase θ is considered. In Eq. 1 the index l labels the different superconducting layers (separated by a distance s), J_{\parallel} and J_{\perp} are the order parameter phase coupling constants within the layers and between different layers (respectively) and the potential vector \mathbf{A}_{\parallel} describes both the magnetic field applied parallel to the c axis and the one induced by thermal fluctuations. The second derivative of the free energy resulting from Eq. 1 yields the field dependent susceptibility $\chi(H)$:

$$\chi(H) = -\frac{k_B T}{\Phi_0^2} \frac{1}{s(1+2n)} \left\{ \frac{\left[1 + \left(\frac{H}{H^*} \right)^2 \delta \right]^2}{n_{vor}} + s^2 \gamma^2 (1+n) n \left[1 + \left(\frac{H}{H^*} \right)^2 \delta \right]^2 \right\} + \frac{47\pi L^2 J_{\parallel}}{540 s} \left(\frac{2\pi}{\Phi_0} \right)^2 \left(\frac{H}{H^*} \right)^2 \delta \quad (2)$$

where $\delta = J_{\parallel}/k_B T$, $H^* \equiv \Phi_0/L^2$ is a characteristic field related to the size L of the islands, while $\gamma \equiv \xi_{ab}(0)/\xi_c(0)$ is the anisotropy factor. In Eq. 2, $n_{vor} = n_H + n_{th}$ is the total vortex density due to the field induced vortices $n_H = H/\Phi_0$ and the thermally excited vortices, whose density n_{th} is affected by the applied field also depending on the number n of correlated layers:

$$n_{th} = n_0 \exp \left\{ -\frac{E_0(1+2n)}{k_B T \left[1 + \left(\frac{H}{H^*} \right)^2 \delta \right]} \right\}. \quad (3)$$

When faced with values of upturn fields H_{up} in the order of 100 to 1000 Oe one has to be careful in the data interpretation, since other mechanisms could possibly lead to the observed phenomenology. In disordered systems such as in Al-doped MgB₂ or YNi₂B₂C, for instance, the average bulk T_c arises from a spatial distribution of local transition temperatures $T_c(\mathbf{r})$ inside the sample.^{37,49} The main effect of inhomogeneity is to induce a precursor diamagnetism above T_c associated with the diamagnetic response of those regions where $T_c(\mathbf{r}) > T_c$ holds locally. Also in this case, high magnetic fields tend to reduce the extra-diamagnetic response above T_c giving rise to an upturn field in the isothermal magnetization curves resulting from a distribution of critical fields $H_{c1}(\mathbf{r})$ as-

sociated to the spatial regions where $T_c(\mathbf{r}) > T_c$. In this case, H_{up} mimics the behaviour of $H_{c1}(T)$.

A straightforward way of distinguishing extra-diamagnetism due to phase fluctuations from precursor diamagnetism due to sample inhomogeneity lies in the different temperature dependence of the upturn field in the two regimes.⁵⁰ H_{up} , in fact, increases on increasing temperature in the phase SF scenario while it decreases in disorder-induced diamagnetism.

IV. EXPERIMENTAL RESULTS

A detailed analysis of the different contributions to the macroscopic magnetization M of the sample together with the procedure to extract M_{dia} from the isothermal magnetization curves will be outlined in the following.

M vs. T curves at small magnetic field ($H = 5$ Oe) obtained both in ZFC and FC conditions are reported in Fig. 1. A slight separation between FC and ZFC data already at $T \gg T_c$ implies the presence of a small amount of spurious magnetic phases. The transition temperature $T_c(H \rightarrow 0) = (52.3 \pm 0.1)$ K can be estimated by first subtracting in a few-K region around the diamagnetic onset a contribution associated with that spurious

magnetic signal (see details subsequently). Then, T_c is evaluated as the intersection of two linear fits of the resulting data (well below and well above T_c , as shown in Fig. 1, inset).

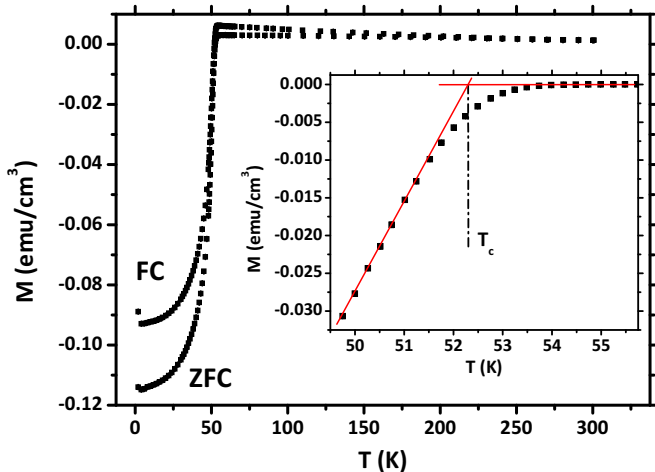


FIG. 1: (Color online) M vs. T magnetization curves in both ZFC and FC conditions at $H = 5$ Oe. Inset: blow up of the onset region in the FC curve after subtracting a linear contribution accounting for other sources of magnetism in this narrow T -range (see text). The superconducting transition temperature can be estimated as $T_c \simeq 52.3$ K.

In Fig. 2 representative raw M vs. T curves at high magnetic fields are shown. The data are well fitted by the phenomenological function

$$M_{dc}(T) = M_{sc} \left[1 - \left(\frac{T}{T_c} \right)^\alpha \right]^\beta + C_{cw} \frac{H}{T - T_N} + M_0. \quad (4)$$

The first term is the diamagnetic Meissner response (which we have empirically fitted by a two-exponents mean field function). The second term in Eq. 4 is the Curie-Weiss paramagnetic contribution associated with the Sm^{3+} sublattice, with $T_N = 4$ K as fixed parameter. The best fit of the Curie-Weiss constant C_{cw} leads to a magnetic moment $\mu = (0.32 \pm 0.01) \mu_B$ per Sm^{3+} ion. This is in close agreement with the value $\mu \simeq 0.53 \mu_B$ reported from a neutron-diffraction experiment in the antiferromagnetically-ordered phase.⁵¹ The tetragonal crystalline electrostatic environment is known to be described in the Stevens' operators formalism as

$$\hat{H}_{CEF} = B_2^0 \hat{O}_2^0 + B_4^0 \hat{O}_4^0 + B_4^4 \hat{O}_4^4 \quad (5)$$

leading in the case of both Sm^{3+} and Ce^{3+} to a splitting of the ground state $J = \frac{5}{2}$ multiplet into three doublets.^{52,53} However, crystal-field effects on the magnetization can be safely disregarded in the examined temperature range ($T < 60$ K), thus justifying the use of a simple Curie-Weiss fitting function for the paramagnetic contribution.⁵²⁻⁵⁵ Finally, the last T -independent

term in Eq. 4 arises from different contributions including a Pauli-like susceptibility associated with itinerant electrons, ionic diamagnetism and a small amount of ferromagnetic impurities. The impurity contribution $M_{imp} \simeq 0.23 \text{ emu/cm}^3$ (saturated value for $H \gtrsim 1$ T) was quantified from a isothermal M vs. H curve at $T = 56$ K and, more precisely, from the intercept value of the linear fit of the paramagnetic contribution at $H = 0$ Oe. The parameters obtained from the fitting procedure at different magnetic fields in the range $1.5 \text{ T} \leq H \leq 7 \text{ T}$ have been reported in Tab. I.

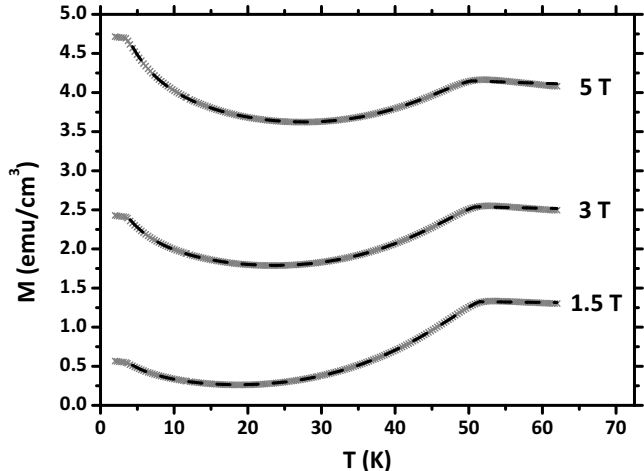


FIG. 2: M vs. T magnetization curves in FC conditions at different magnetic fields. The data are fitted according to a phenomenological expression (Eq. 4, see dashed lines). Low-temperature anomalies ($T \simeq 4$ K) are related to the antiferromagnetic ordering of Sm^{3+} magnetic moments.⁵¹

In order to obtain reliable estimates of the SF diamagnetic contribution M_{dia} , one has to allow for all the additional contributions discussed above. At this aim, we employed the subtraction procedure successfully used in the analysis of cuprate materials and of MgB_2 . Isothermal M vs. H curves ($H < 5$ T) were measured at selected temperatures around the superconducting onset ($50 \text{ K} < T < 56 \text{ K}$) and the high-field linear paramagnetic contribution was individually subtracted from those curves to account for its T -dependence. The so-called reference isothermal curve (relative, in this case, to $T = 56$ K) was then subtracted to each obtained curve. By doing this, one subtracts all the other sources of T -independent magnetism, by considering the fact that the spurious contribution is practically constant in this narrow T range. The reference $T = 56$ K was chosen by carefully examining the onset region in Fig. 1. In particular, a value close enough to the investigated region was selected to neglect the possible T -dependence of spurious contributions, meantime safely far from the fluctuative region itself.

In Fig. 3 representative isothermal magnetization curves M_{dia} vs. H obtained in ZFC conditions at different temperatures above $T_c(H = 0)$ are shown in the

TABLE I: Parameters associated with the fitting procedure of M vs. T curves (see Fig. 2 for representative raw data) at different H values (see first column, units: T) by means of the phenomenological expression reported in Eq. 4. M_{sc}/H quantifies the amplitude of the diamagnetic response from the superconducting phase (units: erg/Oe² cm³), T_c is the superconducting critical temperature (units: K), α and β are the two exponents of the mean-field-like phenomenological contribution representing the superconducting shielding, C_{cw} is the Curie-Weiss constant associated with the paramagnetic phase of the Sm³⁺ sublattice (units: erg K/Oe² cm³) and M_0/H represents all the other sources of T -independent magnetism (units: erg/Oe² cm³).

H	$10^5 M_{sc}/H$	T_c	α	β	$10^5 C_{cw}$	$10^5 M_0/H$
1.5	-7.95	51.28	3.54	1.19	25.26	8.34
2	-5.42	51.145	3.68	1.22	24.66	8.13
2.5	-3.98	51.05	3.82	1.25	24.39	8.10
3	-3.11	50.96	3.97	1.29	24.09	8.02
3.5	-2.49	50.89	4.09	1.33	23.93	8.02
4	-2.07	50.815	4.24	1.37	23.68	7.97
5	-1.51	50.675	4.47	1.44	23.33	7.88
6	-1.16	50.545	4.69	1.51	23.01	7.75
7	-0.93	50.43	4.94	1.59	22.76	7.62

low-field range (up to $H \simeq 1000$ Oe). From the analysis of the data interesting insights are obtained. One notices the appearance of upturn fields in the order of 200 to 400 Oe. More interestingly, it is noted (see Fig. 3, inset) that, in the temperature limit $T > T_c$, H_{up} increases on increasing temperature. As emphasized in Sect. III, both the small values of H_{up} and the increase of H_{up} on increasing temperature suggest that the observed diamagnetism above T_c can be ascribed to the presence of phase SF. The effects of the $T_c(\mathbf{r})$ distribution, due to some sample inhomogeneity, can safely be neglected. This does not imply that the sample is totally homogeneous but rather that the phase fluctuations play a dominant role in the diamagnetism above T_c at the examined fields.

In SmFeAsO_{0.8}F_{0.2} the value of the coherence length is still controversial. By examining paraconductivity data, analyzed with a four-band three-dimensional model, one derives $\xi_0 = 19$ Å,⁵⁶ while using a two-dimensional lowest Landau level scaling and H_{c2} measurements in single-crystal samples the same quantity ranges from 3 to 4 Å.^{57,58} Thus, the estimated values for ξ_0 are anyway small, in analogy with those found in cuprate materials. Then, in the framework of classical GL fluctuations for $\epsilon \sim 10^{-2}$, H_{up} would be expected to vary between 5 T and 25 T. It is evident that the occurrence of an upturn field of the order of few hundred Gauss in the magnetization curves of Fig. 3 cannot be ascribed to the saturation of magnetization expected in GL fluctuations regime.

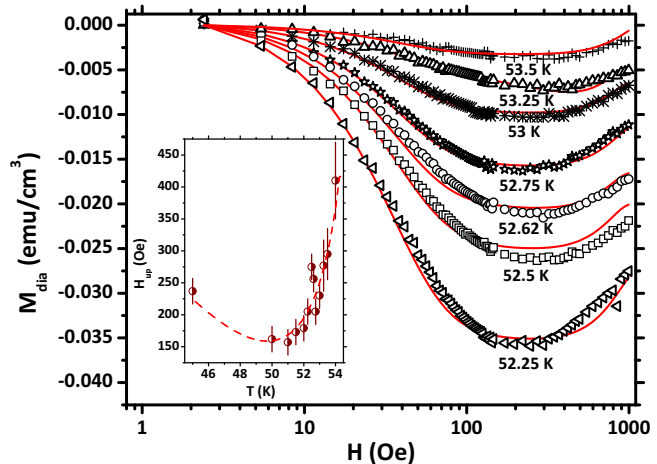


FIG. 3: (Color online) Isothermal diamagnetic contributions M_{dia} vs. H for representative temperatures above T_c , displaying upturn fields in the range $H_{up} \sim 200$ to 400 Oe. The curves have been obtained after the subtraction procedure described in the text. Continuous lines are best-fits obtained by means of numerical integration of Eq. 2. Inset: temperature dependence of the upturn field, clearly increasing on increasing T above T_c . The dashed line is a guide for the eye.

V. DISCUSSION AND CONCLUSIONS

By means of numerical integration of Eq. 2, the magnetization curves as a function of field are obtained (solid lines in Fig. 3). The parameters corresponding to the best fit are collected in Tab. II. The interlayer distance has been set $s = 8.5$ Å.

TABLE II: Values of H^* and of the size of the superconducting islands L resulting from the best-fit procedures. The parameter N should be considered an order-of-magnitude estimate of the number of islands having assumed superconducting regions of volume given by $L^2 d$ with the value of the depth d fixed to 25.5 Å (corresponding to $n = 3$, see text).

T (K)	H^* (Oe)	L (nm)	N (cm ⁻³)
52.25	883	154	$2.4 \cdot 10^{14}$
52.5	888	153	$1.5 \cdot 10^{14}$
52.62	1001	145	$1.45 \cdot 10^{14}$
52.75	1101	138	$1.25 \cdot 10^{14}$
53	1360	124	$1 \cdot 10^{14}$
53.25	1440	121	$5.2 \cdot 10^{13}$
53.5	1581	115	$4.9 \cdot 10^{13}$

According to the relation $n_0 \simeq 10^4/a^2$, in Eq. 3 one has $n_0 = 6.5 \cdot 10^{18}$ cm⁻², for $a = 3.9$ Å.³¹ The activation energy E_0 in Eq. 3 is usually estimated around $10 k_B T_c$ then the term $E_0 (1 + 2n)$, chosen as a free parameter, allows an evaluation of n . In particular, $E_0 (1 + 2n) = 28 k_B T_c$ indicating the number of correlated layers $n = 3$,

with an activation energy $E_0 \simeq 4 k_B T_c$. Similar investigations in YBCO²⁴ and in Sm-based cuprates⁴³ have been performed using $n = 3$, in agreement with the fact that all these systems have similar anisotropy parameters. For this reason in this analysis $\gamma = 7$ will be considered as a working hypothesis. Furthermore, $E_0 (1 + 2n)$ turns out almost temperature independent, suggesting that the number of correlated layers does not appreciably change in the temperature range that has been studied. In the numerical integration procedure also H^* and $J_{\parallel}/k_B T$ are given as free parameters. From the characteristic field H^* it is possible to estimate an order of magnitude of the average size L of the superconducting regions (see Tab. II).

As might be expected, on increasing temperature the areas with non-zero order parameter progressively reduce in size. The progressive decrease of the volume occupied by the superconducting regions are due both to the decrease in the average size of the islands and/or to the decrease of their number.

The term $J_{\parallel}/k_B T$ results nearly independent on temperature, around the value 2.5. In other situations, as in Sm based cuprates,⁴³ this ratio decreases with increasing temperature, according to its close relation to the superfluid density, as suggested by the Berezinskii-Kosterlitz-Thouless theory.²¹ In the present case the fluctuation effect can be detected in a temperature range too small to appreciate the reduction.

A further confirmation of the inapplicability of the conventional GL model, at least in the field range of Fig. 3, can be drawn from analysis of the reduced magnetization $m_c = M_{dia}/\sqrt{HT_c}$ vs. T , shown in Figs. 4 and 5. The data have been obtained by considering M vs. T curves at different magnetic fields in the range $0 < H < 7$ T (like those shown in Fig. 2) and by individually subtracting a linear contribution in a few-K region around the onset to each curve accounting for all sources of magnetism other than Meissner shielding and SF effects (as described in Sect. IV).

According to the GL theory for gaussian fluctuations and scaling arguments for isotropic superconductors, m_c should take the universal value^{21,38,59,60}

$$m_c = \frac{k_B}{\Phi_0^{3/2}} m_3(\infty) \simeq 4.6 \cdot 10^{-7} \text{ emu/cm}^3 \text{ Oe}^{1/2} \text{ K} \quad (6)$$

at $T \simeq T_c$ where the experimental data should cross. If the system is anisotropic, the value of m_c is expected to be enhanced by a factor γ . In Fig. 4 no crossing in m_c vs. T data is observed at fields up to 1.5 T, in contrast with the scaling prediction. Conversely, Fig. 5 shows that at higher fields, up to 7 T, the reduced magnetization curves as a function of temperature cross at $T = 53.2$ K assuming the value $m_c \simeq 2.7 \cdot 10^{-7} \text{ emu/cm}^3 \text{ Oe}^{1/2} \text{ K}$. Since the data refer to powders, the value of m_c must be multiplied by a factor 3, which takes into account the powder average, as shown elsewhere in the case of MgB₂.^{23,35} An anisotropy parameter $\gamma \sim 2$ would then be inferred. This value is smaller than the ones re-

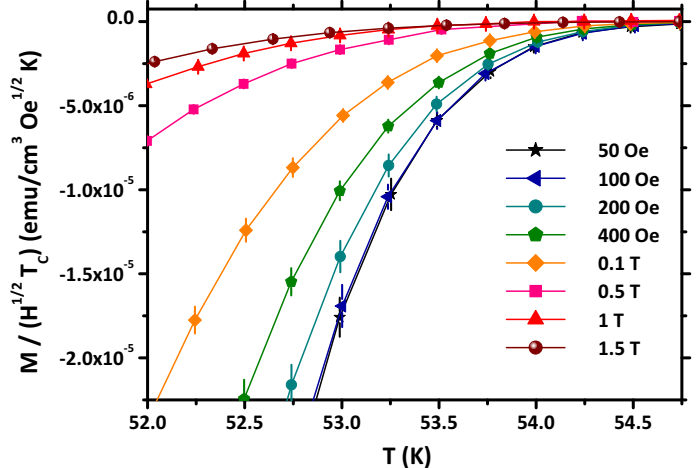


FIG. 4: (Color online) Reduced magnetization $m_c = M_{dia}/\sqrt{HT_c}$ vs. T at magnetic fields $H \leq 1.5$ T. No crossing of curves at T_c is observed.

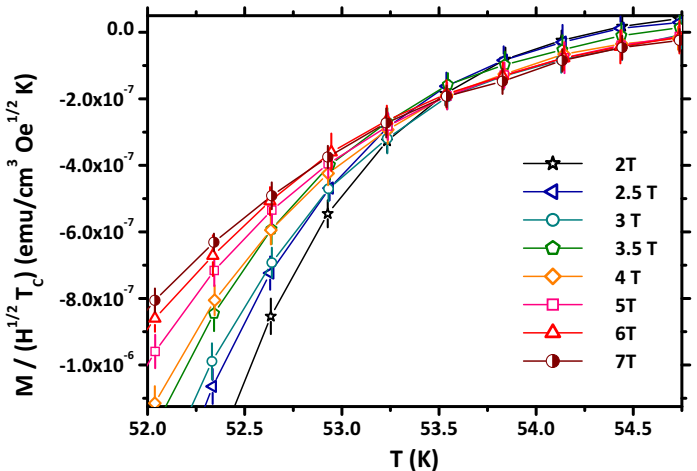


FIG. 5: (Color online) Reduced magnetization $m_c = M_{dia}/\sqrt{HT_c}$ vs. T at magnetic fields $H \geq 2$ T. Crossing of curves at $T \simeq 53.2$ K suggests that the classical GL framework is applicable at high fields, where the contribution from phase fluctuations is suppressed.

ported in literature ($\gamma = 5$ to 9) which however show large uncertainty and appear to be related to the doping level.^{57,58} Furthermore, the crossing temperature is slightly above the critical temperature estimated from the inset of Fig. 1. These aspects are possibly due to the renormalization of the transition temperature due to the phase fluctuations.⁶¹ The effects related to the simultaneous occurrence of non-conventional phase fluctuations and GL classical fluctuations are worthy of further experimental and theoretical studies. In conclusion, it appears that the fluctuation diamagnetism above T_c can be described by GL theory only at high fields, while at a lower field range the phenomena highlighted in Fig. 3 require

a different explanation based on the occurrence of phase-fluctuations.

Summarizing, the diamagnetic response above T_c at low magnetic field in $\text{SmFeAsO}_{0.8}\text{F}_{0.2}$ cannot be described within the classical Ginzburg-Landau approach. From this point of view, the system is not comparable either to BCS superconductors or to optimally-doped cuprates. On the contrary, the experimental results support the picture based on the idea of precursor islands where the amplitude of the order parameter is frozen, while the long-range coherence associated with a bulk superconducting state is prevented by marked fluctuations in the phase.

Acknowledgments

Stimulating discussions with P. Carretta and A. Varlamov are gratefully acknowledged. A. Palenzona is acknowledged for the sample preparation. One of us (G. P.) thanks E. Bernardi for an early collaboration on fluctuating diamagnetism in metallic nanoparticles and useful discussions concerning data analysis.

This work was partially supported by Compagnia di S. Paolo and by MIUR under Project No. PRIN2008XWLWF9.

-
- ¹ Y. Kamihara, T. Watanabe, M. Hirano, H. Hosono, *J. Am. Chem. Soc.* **130**, 3296 (2008)
 - ² H. D. Lumsden and A. D. Christianson, *J. Phys.: Cond. Matt.* **22**, 203203 (2010)
 - ³ D. C. Johnston, *Adv. Phys.* **59**, 803 (2010)
 - ⁴ C.-T. Chen, C. C. Tsuei, M. B. Ketchen, Z.-A. Ren, Z. X. Zhao, *Nature Phys.* **6**, 260 (2010)
 - ⁵ K. Nakayama, T. Sato, P. Richard, Y.-M. Xu, Y. Sekiba, S. Souma, G. F. Chen J. L. Luo, N. L. Wang, H. Ding, T. Takahashi, *Europhys. Lett.* **85**, 67002 (2009)
 - ⁶ M. Iavarone, G. Karapetrov, A. E. Koshelev, W. K. Kwok, G. W. Crabtree, D. G. Hinks, W. N. Kang, E.-M. Choi, H.-J. Kim, H.-J. Kim, S. I. Lee, *Phys. Rev. Lett.* **89**, 187002 (2002)
 - ⁷ I. I. Mazin, D. J. Singh, M. D. Johannes, M. H. Du, *Phys. Rev. Lett.* **101**, 057003 (2008)
 - ⁸ G. A. Ummarino, M. Tortello, D. Daghero, R. S. Gonnelli, *Phys. Rev. B* **80**, 172503 (2009)
 - ⁹ D. Daghero, M. Tortello, R. S. Gonnelli, V. A. Stepanov, N. D. Zhigadlo, J. Karpinski, *Phys. Rev. B* **80**, 060502(R) (2009)
 - ¹⁰ H.-S. Lee, M. Bartkowiak, J. S. Kim, H.-J. Lee, *Phys. Rev. B* **82**, 104523 (2010)
 - ¹¹ G. Prando, P. Carretta, R. De Renzi, S. Sanna, A. Palenzona, M. Putti, M. Tropeano, *Phys. Rev. B* **83**, 174514 (2011)
 - ¹² G. Blatter, M. V. Feigel'man, V. B. Geshkenbein, A. I. Larkin, V. M. Vinokur, *Rev. Mod. Phys.* **66**, 1125 (1994)
 - ¹³ R. H. Koch, V. Foglietti, W. J. Gallagher, G. Koren, A. Gupta, M. P. A. Fisher, *Phys. Rev. Lett.* **63**, 1511 (1989)
 - ¹⁴ D. S. Fisher, M. P. A. Fisher, D. A. Huse, *Phys. Rev. B* **43**, 130 (1991)
 - ¹⁵ P. Cheng, H. Yang, Y. Jia, L. Fang, X. Zhu, G. Mu, H. H. Wen, *Phys. Rev. B* **78**, 134508 (2008)
 - ¹⁶ T. Sato, S. Souma, K. Nakayama, K. Terashima, K. Sugawara, T. Takahashi, Y. Kamihara, M. Hirano, H. Hosono, *Journ. Phys. Soc. Jpn.* **B 77**, 063708 (2008)
 - ¹⁷ T. Mertelj, V. V. Kabanov, C. Gadermaier, N. D. Zhigadlo, S. Katrych, J. Karpinski, D. Mihailovic, *Phys. Rev. Lett.* **102**, 117002 (2009)
 - ¹⁸ R. S. Gonnelli, D. Daghero, M. Tortello, G. A. Ummarino, V. A. Stepanov, J. S. Kim, and R. K. Kremer, *Phys. Rev. B* **79**, 184526 (2009)
 - ¹⁹ I. Pallicchi, M. Tropeano, C. Ferdeghini, G. Lamura, A. Martinelli, A. Palenzona, M. Putti, *J. Supercond. Nov. Magn.*, in press
 - ²⁰ W. J. Skocpol, M. Tinkham, *Rep. Prog. Phys.* **B 38**, 1049 (1975)
 - ²¹ M. Tinkham, *Introduction to Superconductivity*, McGraw-Hill Book Co. (1996)
 - ²² A. Larkin, A. Varlamov, *Theory of Fluctuations in Superconductors*, Oxford Science Publications (2005)
 - ²³ A. Lascialfari, T. Mishonov, A. Rigamonti, P. Tedesco, A. Varlamov, *Phys. Rev. B* **65**, 180501(R) (2002)
 - ²⁴ A. Lascialfari, A. Rigamonti, L. Romanó, P. Tedesco, A. Varlamov, D. Embriaco, *Phys. Rev. B* **65**, 144523 (2002)
 - ²⁵ J. M. Murray, Z. Tesanovic, *Phys. Rev. Lett.* **105**, 037006 (2010)
 - ²⁶ U. Welp, C. Chaparro, A. E. Koshelev, W. K. Kwok, A. Rydh, N. D. Zhigadlo, J. Karpinski, S. Weyeneth, *Phys. Rev. B* **83**, 100513 (2011)
 - ²⁷ J. Mosqueira, J. D. Dancausa, F. Vidal, S. Salem-Sugui Jr., A. D. Alvarenga, H.-Q. Luo, Z.-S. Wang, H.-H. Wen, *Phys. Rev. B* **83**, 094519 (2011)
 - ²⁸ A. Sewer, H. Beck, *Phys. Rev. B* **64**, 014510 (2001)
 - ²⁹ L. Romanó, *Int. Journ. Mod. Phys. B* **17**, 423 (2003)
 - ³⁰ A. Martinelli, M. Ferretti, P. Manfrinetti, A. Palenzona, M. Tropeano, M. R. Cimberle, C. Ferdeghini, R. Valle, C. Bernini, M. Putti, A. S. Siri, *Supercond. Sci. Technol.* **21**, 095017 (2008)
 - ³¹ S. Margadonna, Y. Takabayashi, M. T. McDonald, M. Brunelli, G. Wu, R. H. Liu, X. H. Chen, K. Prassides, *Phys. Rev. B* **79**, 014503 (2009)
 - ³² G. Prando, P. Carretta, A. Rigamonti, S. Sanna, A. Palenzona, M. Putti, M. Tropeano, *Phys. Rev. B* **81**, 100508(R) (2010)
 - ³³ A. E. Koshelev, *Phys. Rev. B* **50**, 506 (1994)
 - ³⁴ M. A. Hubbard, M. B. Salamon, B. W. Veal, *Physica C* **259**, 309 (1995)
 - ³⁵ T. Mishonov, E. Penev, *Int. Journ. Mod. Phys. B* **14**, 3831 (2000)
 - ³⁶ L. Romanó, A. Lascialfari, A. Rigamonti, I. Zucca, *Phys. Rev. Lett.* **94**, 247001 (2005)
 - ³⁷ E. Bernardi, A. Lascialfari, A. Rigamonti, L. Romanó, *Phys. Rev. B* **77**, 064502 (2008)
 - ³⁸ A. Junod, J.-Y. Genoud, G. Triscone, T. Schneider, *Physica C* **294**, 115 (1998)
 - ³⁹ E. Bernardi, A. Lascialfari, A. Rigamonti, L. Romanó, V. Iannotti, G. Ausanio, C. Luponio, *Phys. Rev. B* **74**, 134509 (2006)

- ⁴⁰ A. Lascialfari, A. Rigamonti, P. Tedesco, L. Romanó, A. Varlamov, D. Embriaco, *Int. Journ. Mod. Phys. B* **17**, 785 (2003)
- ⁴¹ A. Lascialfari, A. Rigamonti, L. Romanó, A. A. Varlamov, I. Zucca, *Phys. Rev. B* **68**, 100505(R) (2003)
- ⁴² L. Li, Y. Wang, S. Komiya, S. Ono, Y. Ando, G. D. Gu, N. P. Ong, *Phys. Rev. B* **81**, 054510 (2010)
- ⁴³ E. Bernardi, A. Lascialfari, A. Rigamonti, L. Romanó, M. Scavini, C. Oliva, *Phys. Rev. B* **81**, 064502 (2010)
- ⁴⁴ V. J. Emery, S. A. Kivelson, *Nature* **374**, 434 (1995)
- ⁴⁵ Z. A. Xu, N. P. Ong, Y. Wang, T. Kakeshita, S. Uchida, *Nature* **406**, 486 (2000)
- ⁴⁶ I. Iguchi, T. Yamaguchi, A. Sugimoto, *Nature* **412**, 420 (2001)
- ⁴⁷ K. M. Lang, V. Madhavan, J. E. Hoffman, E. W. Hudson, H. Eisaki, S. Uchida, J. C. Davis, *Nature* **415**, 412 (2002)
- ⁴⁸ Y. Wang, L. Li, N. P. Ong, *Phys. Rev. B* **73**, 024510 (2006)
- ⁴⁹ L. Cabo, F. Soto, M. Ruibal, J. Mosqueira, F. Vidal, *Phys. Rev. B* **73**, 184520 (2006)
- ⁵⁰ A. Rigamonti, A. Lascialfari, L. Romanó, A. Varlamov, I. Zucca, *J. Supercond. Incorp. Nov. Magn.*, DOI:10.1007/s10948-005-0077-z
- ⁵¹ D. H. Ryan, J. M. Cadogan, C. Ritter, F. Canepa, A. Palenzona, M. Putti, *Phys. Rev. B* **80**, 220503(R) (2009)
- ⁵² J. H. Van Vleck, *The Theory of Electric and Magnetic Susceptibilities*, Oxford University Press (1932)
- ⁵³ S. Chi, D. T. Adroja, T. Guidi, R. Bewley, S. Li, J. Zhao, J.W. Lynn, C. M. Brown, Y. Qiu, G. F. Chen, J. L. Lou, N. L. Wang, P. Dai, *Phys. Rev. Lett* **101** 217002 (2008)
- ⁵⁴ P. J. Baker, S. R. Giblin, F. L. Pratt, R. H. Liu, G. Wu, X. H. Chen, M. J. Pitcher, D. R. Parker, S. J. Clarke, S. J. Blundell, *New Journ. Phys.* **11** 025010 (2009)
- ⁵⁵ M. R. Cimberle, F. Canepa, M. Ferretti, A. Martinelli, A. Palenzona, A. S. Siri, C. Tarantini, M. Tropeano, C. Ferdeghini, *Journ. Magn. Magn. Mat.* **321** 3024 (2009)
- ⁵⁶ L. Fanfarillo, L. Benfatto, S. Caprara, C. Castellani, M. Grilli, *Phys. Rev. B* **79**, 172508 (2009)
- ⁵⁷ I. Pallecchi, C. Fanciulli, M. Tropeano, A. Palenzona, M. Ferretti, A. Malagoli, A. Martinelli, I. Sheikin, M. Putti, C. Ferdeghini, *Phys. Rev. B* **79**, 104515 (2009)
- ⁵⁸ H.-S. Lee, M. Bartkowiak, J.-H. Park, J.-Y. Lee, J.-Y. Kim, N.-H. Sung, B. K. Cho, C.-U. Jung, J. S. Kim, H.-J. Lee, *Phys. Rev. B* **80**, 144512 (2009)
- ⁵⁹ T. Schneider, H. Keller, *Physica C* **207**, 366 (1993)
- ⁶⁰ T. Schneider, H. Keller, *Int. Journ. Mod. Phys. B* **8**, 487 (1994)
- ⁶¹ J. L. Tallon, J. G. Storey, J. W. Loram, *Phys. Rev. B* **83**, 092502 (2011)